Spatially Resolved Vibrational Energy Transfer in Molecular Monolayers

Jeffrey A. Carter, Zhaohui Wang, and Dana D. Dlott*

School of Chemical Sciences, University of Illinois at Urbana−Champaign, Chemical and Life Sciences Laboratory, 600 South Mathews Avenue, Urbana, Illinois 61801

Received: January 11, 2008

We have shown that it is possible to input heat to one location of a molecule and simultaneously measure its arrival in real time at two other locations, using an ultrafast flash-thermal conductance technique. A femtosecond laser pulse heats an Au layer to ∼800 °C, while vibrational sum-frequency generation spectroscopy (SFG) monitors heat flow into self-assembled monolayers (SAMs) of organic thiolates. Heat flow into the SAM creates thermally induced disorder, which decreases the coherent SFG signal from the CH-stretching transitions. Recent improvements in the technique are described, including the use of nonresonant background-suppressed SFG. The improved apparatus was characterized using alkanethiolate and benzenethiolate SAMs. In the asymmetric 2-methyl benzenethiolate SAM, SFG can simultaneously monitor CH-stretching transitions of both phenyl and methyl groups. The phenyl response to flash-heating occurs at least as fast as the 1 ps time for the Au surface to heat. The methyl response has a faster portion similar to the phenyl response and a slower portion characterized by an 8 ps time constant. The faster portions are attributed to disordering of the methyl-substituted phenyl rings due to thermal excitation of the Au−S adbonds. The slower portion, seen only in the methyl SFG signal, is attributed to heat flow from the metal surface into the phenyl rings and then to the methyl groups.

Introduction

In this study, we showed that it is possible to input vibrational energy to one location of a molecule and then simultaneously measure the different arrival times for vibrational energy at two other locations of the same molecule. This study uses an improved version of the ultrafast flash-thermal conductance technique described recently.[1,2] In this technique, depicted in Figure 1a, a metal thin film with an adsorbed self-assembled molecular monolayer (SAM) was flash-heated by a femtosecond laser pulse to a high temperature several hundreds of degrees Kelvin above ambient temperature. The resulting heat flow from the metal layer into the adsorbed SAM via the thiolate−gold adbond was monitored using time-resolved broad-band multiplex vibrational sum-frequency generation (SFG) spectroscopy[3] to probe vibrational transitions of the SAM molecules.[1,2] Previous studies of heat flow across bridged azulenes include work by Schwarzer et al.,[4,5] heat flow into Langmuir Blodget thin films by Zewail et al.,[6−8] and T-jump SFG studies of surfactants by Bonn et al.[9] The SAM studied here consists of 2-methyl benzene thiolate (2MBT) on polycrystalline Au(111). For reference, experiments also were performed on a 16 carbon alkanethiolate (C16 AT), benzenethiolate (BT), and 4- and 3-methyl benzenethiolate (4MBT and 3MBT). In the 2MBT system, it is possible for SFG to monitor CH-stretching transitions of both the phenyl ring and the methyl substituent. This two-point monitoring of ultrafast molecular heat flow represents a significant advance over our previous work.

Vibrational energy flow in molecules remains a difficult problem in physical chemistry and has received new attention in the context of molecular electronics and molecular wires.[10−15] Most studies of vibrational energy treat the process in an energy level picture. By this, we mean experiments and theory that investigate the rates of energy flow between or among various vibrational energy levels. This type of picture emerges naturally from quantum mechanics and vibrational spectroscopy because both focus on molecular energy levels and transitions. An alternative picture of vibrational energy is based on the motion of localized energy wavepackets that propagate in time and space from one part of a molecule to another. This type of location picture seems more intuitive, and it helps to answer questions such as how is heat transported across molecular wires or how does energy flow through a molecule to chemically activate the breaking of a specific chemical bond? The location

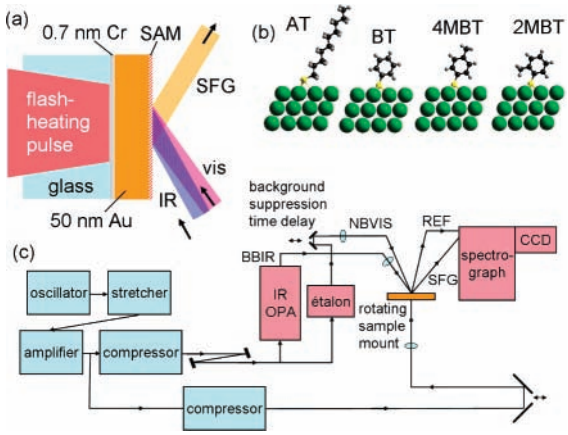

Figure 1. (a) Schematic of ultrafast flash-thermal conductance measurements. After flash-heating the metal surface by several hundreds of degrees Kelvin, thermally induced disorder of the SAM was probed by ultrafast vibrational SFG spectroscopy. (b) Molecular structures studied in this work. All samples consist of closely packed 2-D SAM lattices. About 10^{11} molecules were probed on each laser shot. Key: AT = alkanethiolate; BT = benzenethiolate; 4MBT = 4-methyl benzenethiolate; and 2MBT = 2-methyl benzenethiolate. (c) Schematic of laser setup using picosecond NBVIS and femtosecond BBIR pulses to generate a reference SFG signal from the metal layer and a vibrationally resonant SFG signal from the SAM.

10.1021/jp800278c CCC: $40.75
Published on Web 03/18/2008

picture emerges naturally from measurements that study the dynamics of local mode excitations or from nonequilibrium molecular dynamics (MD) simulations of energy flow from initially localized excitations.[16−18] Ordinarily, measurements of this type see only the movement of energy out of the initial localized state. Examples of this are numerous, including classics such as Smalley et al.'s study of intramolecular vibrational relaxation in alkyl benzenes,[19] where the fluorescence lineshapes of phenyl vibronic transitions were observed to broaden as progressively longer alkyl groups were attached, the vibrational relaxation of CH-stretching overtones of benzene by Reddy et al.,[20] and the relaxation of OH-stretch on silica surfaces by Heilweil and co-workers.[21] Recently, there have been reports of techniques that simultaneously probe the loss of vibrational energy from one location and the arrival of a part of that energy at a different location,[22] for instance, our group's study of liquid state alcohols[23] OH-$(CH_2)_n$-CH_3, where energy transfer from OH to CH_3, via intervening CH_2 groups, was monitored by IR-Raman analysis.

In previous works using the ultrafast flash-thermal conductance method,[1,2] we studied heat transport along AT molecular wires[10,11] having an even number of carbon atoms ranging from six to 24,[2] as well as heat flow into BT and the closely related benzyl mercaptide (-S-CH_2-C_6H_5).[1] In the AT experiments, laser flash-heating jumped the temperature of the metal substrate to ~800 °C in 1 ps, while SFG was used to monitor CH-stretching transitions (~2950 cm^{-1}) of the terminal methyl groups. Heating may affect the SFG spectrum in different ways: the spectral transitions may broaden, shift, or lose intensity.[1] We ordinarily focus on the intensity loss because it is easiest to measure.[1,2,24,25] In AT, which forms densely packed highly ordered 2-D lattices,[26,27] the loss of coherent SFG intensity resulted from thermally induced disordering of these methyl groups.[2]

We (and others[28−30]) have found that the time constant τ for the heating of adsorbed AT SAM molecules on hot metal surfaces is generally controlled by the strength of coupling between the metal phonons and the AT SAM vibrations. This coupling strength is characterized by the interface thermal conductance,[2,31] G. The time constant τ is related to G by[2]

$$G = \rho h C_p/\tau \quad (1)$$

where ρ is the SAM density, h is the height of the SAM above the surface, and C_p is the SAM specific heat. In the limit of long alkane chains where end effects can be ignored, one would expect the interface conductance G in eq 1 to be independent of chain length. Since, in this limit, C_p is a linearly increasing function of chain length, eq 1 suggests that τ also should increase linearly with chain length, which indeed was the case.[2] In other words, at constant G, longer AT chains heat up more slowly. More heat must be transported across the interface to raise the temperature of a longer chain with its greater thermal mass. Our measurements yielded[2] $G = 220$ (±100) MW m^{-2} K^{-1}. Using an area per alkane chain of $\rho h = 2.2 \times 10^{-19}$ m^2,[32] the thermal conductance per AT molecule was determined to be 50 pW K^{-1}, which equals 0.3 eV ns^{-1} K^{-1}. These values were similar to what was previously obtained in studies of SAM-decorated Au nanoparticles in aqueous solutions[33] and to what was predicted theoretically by Nitzan and co-workers.[10,11]

Our experiments also revealed a feature not seen previously, which resulted from our unique combination of high time and space resolution. It was possible to measure the propagation delay of the leading edge of the heat burst as it moved from the metal surface, through the alkane chain, to the terminal methyl groups.[1,2] We found that this propagation delay increased linearly with alkane chain length, indicating that the initial stages of heat flow along the AT chains were characterized by ballistic motion. Analysis of the propagation delay versus chain length yielded a velocity of 1 km/s.[1,2] This velocity, which is quite a bit slower than the ~2.5 km/s speed of sound in hydrocarbon oils or polyethylene, was interpreted as the thermally averaged group velocity of the AT molecular vibrations that transport heat along the chains.[2,10,11,15] These vibrations have a lower group velocity than the acoustic phonons that transport heat in bulk media. Finally, we found that energy transfer from the hot Au surface to AT chains generated vibrational excitations initially localized on segments near the base of the AT chains that were ~0.8 nm in length.[2] In other words, the hot Au surface couples not to the SAM's thiolate linkage (Au−S−CH_2-...) alone but to a base region of the AT chains −four to five carbon atoms in length.[2]

In this work, we extended these techniques to study the methyl-substituted BT absorbates shown in Figure 1b. The figures show only a single molecule for clarity, but our measurements look at a region of the 2-D SAM layer containing ~10^{11} molecules within an ~200 μm diameter spot.[2]

Our latest experiments have benefited from several recent improvements discussed next. In particular, we developed a method that allows us to deeply suppress the nonresonant (NR) SFG background signal[34] from the metal layer. In previous works,[1,2,24,25,35,36] this NR background, which was quite a bit larger than the resonant (R) ν_{CH} contribution,[3,37] significantly hindered our ability to measure the ultrafast dynamics of adsorbed monolayers.

The overall time constant for adsorbate heating appears to depend mostly on the interface conductance and molecular heat capacity, so this time constant will not be the quantity of primary interest here. It is the short-time transients showing how the early stages of heat flow propagate through the molecules, and the detection of the arrival of heat at different locations within individual molecules, that will be the focus of the present study.

Vibrational SFG: Time, Frequency, and Space

In this section, we discuss features of background-suppressed broad-band multiplex SFG needed to understand our results. This technique uses two time co-incident pulses produced from an amplified femtosecond Ti:sapphire laser with an optical parametric amplifier (OPA). These are a femtosecond broad-band IR pulse (BBIR) and a picosecond time asymmetric narrow-band visible (NBVIS) pulse. The SFG signal was detected using a spectrograph and multichannel CCD detector. The spectral range encompassed by the BBIR pulses, which for CH-stretching transitions is ~250 cm^{-1} in width centered near 3.3 μm, determines as to which vibrational transitions are probed. The NBVIS pulses in concert with the spectrograph determine the spectral resolution.

SFG is a second-order nonlinear process that depends on the second-order nonlinear susceptibility $\chi^{(2)}$, which in turn depends on the ensemble-averaged molecular first hyperpolarizability.[38−40] In the dipole approximation, the hyperpolarizability factors into a dipole moment and a linear polarizability, so that SFG is characterized by a time correlation function[41] $C(t) = \langle \mu(0)\alpha(t)\rangle$. When a BBIR pulse is incident on a sample, the polarization created in the sample has two contributions

$$P^{IR}(t) = P^{IR}{}_{NR}(t) + P^{IR}{}_{R}(t) \quad (2)$$

where in our sample materials, the NR part arises primarily from the metal surface and the R part from molecular vibrations with nonvanishing IR transition dipole moments. The vibrational

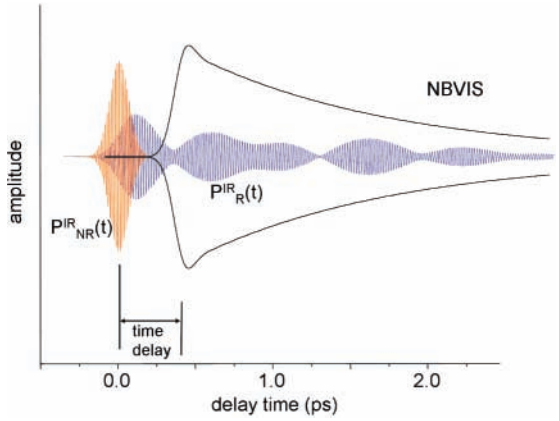

Figure 2. SFG NR background suppression by a time asymmetric picosecond NBVIS. The BBIR pulse duration was about 200 fs. The BBIR pulse created a material polarization that underwent a FID. The FID has a short-lived NR part $P_{IR}^{NR}(t)$, which closely tracks the BBIR pulse, and a long-lived $P_{IR}^{R}(t)$ part due to the SAM vibrational resonances. This polarization interacts with the NBVIS pulse to generate SFG. For clarity, the electric-field oscillations of the NBVIS pulse are not depicted. Time-delaying the NBVIS pulse suppresses the NR signal without significantly reducing the R signal.

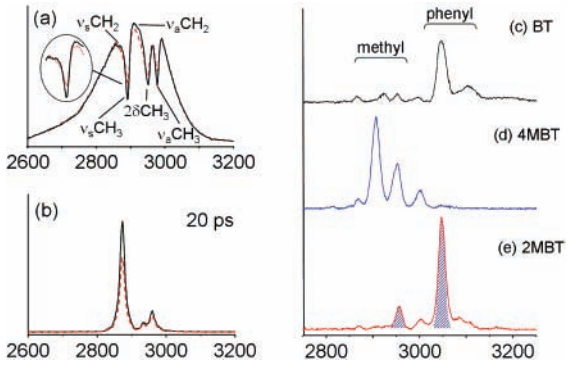

Figure 3. (a) and (b) SFG spectra of AT monolayer on Au(111) with no T-jump (solid lines) and 20 ps after T-jump to ~800 °C (dashed lines). (a) Without NR suppression and (b) with NR suppression. (c–e) SFG spectra of BT, 4MBT, and 2MBT. With 2MBT, both methyl and phenyl transitions (shaded regions in panel e) can be observed.

polarization undergoes a free-induction decay (FID). As depicted in Figure 2, the NR part of the FID decays rapidly, whereas the R part maintains a coherence on the time scale of a few multiples of T_2, the vibrational dephasing time constant.[34] The FID in Figure 2 was computed[34] for the three CH-stretching transitions of an AT terminal methyl group against an Au substrate, using measured parameters for the NR and R amplitudes and the R frequencies and linewidths extracted from spectra such as Figure 3a. The resonant CH-stretching linewidths were $\Delta\nu \approx 8$ cm^{-1}. Since $\Delta\nu = (\pi T_2)^{-1}$, for the methyl CH-stretching transitions, $T_2 \approx 1.3$ ps. (In ref 34, T_2 was given as ~0.7 ps; the value given here is based on a more accurate measurement.)

If the NBVIS pulse is present during the FID, a coherent SFG signal will be generated. In the dipole approximation, this process is formally the same as coherent anti-Stokes Raman scattering.[38] Only vibrational transitions that are both IR and Raman active will contribute to SFG.[39,42,43] Our innovation was to use a time asymmetric visible pulse to suppress the NR background by time windowing.[34] The NBVIS pulses were created by filtering ~100 fs broad-band 800 nm pulses with a Fabry–Perot étalon having a 10 μm air-gap. When a femtosecond pulse is incident upon this étalon, the transmitted pulse has an ~100 fs rise and a slower (~1 ps) exponential ring-down. Because the pulse in space is a packet ~50 μm in length, and the étalon air spacing is 10 μm, the transmitted pulse is not a repetitive train of discrete pulses[34] but instead is decaying almost smoothly. A straightforward computation of the temporal envelope of this NBVIS pulse can be made,[34] as shown in Figure 2. The measured spectral lineshape[34] of the NBVIS pulse is quite close to a Lorentzian with 10.3 cm^{-1} fwhm since the Gaussian temporal component that defines the fast rising edge is just a small part of the total amplitude. As indicated in Figure 2, when the time asymmetric NBVIS pulse is delayed a few hundred femtoseconds after $t = 0$, the NR contribution will be strongly suppressed, with little suppression of the R part.[34]

Usually, the SFG intensity is thought to be proportional to the square of the number density N of molecules or excitations, but this is not always the case when both R and NR components are present

$$I_{SFG} \propto \left|\chi_{NR}^{(2)} + \chi_{R}^{(2)}\right|^2 = \left|\chi_{NR}^{(2)}\right|^2 + \left|\chi_{R}^{(2)}\right|^2 + 2\left|\chi_{NR}^{(2)}\chi_{R}^{(2)}e^{i\delta}\right| \quad (3)$$

where δ is the phase difference, and ignoring orientational averaging, the susceptibility χ is proportional to N. When the NR background is large, $\chi_R^{(2)} \ll \chi_{NR}^{(2)}$, the cross-term dominates, and $I_{SFG} \propto N$. When the background is small or absent, $\chi_R^{(2)} \gg \chi_{NR}^{(2)}$, and $I_{SFG} \propto N^2$. In ordinary SFG measurements of SAMs on metal surfaces, the intermediate situation where $\chi_R^{(2)} \approx \chi_{NR}^{(2)}$ is usually the case, and in this situation, I_{SFG} is proportional to N raised to a power between one and two,[44] and the precise value of this power will vary with time as the R amplitude changes during the flash-heating process.

In our original measurements without background suppression, fluctuations in the background were the major impediment to data analysis. With a high degree of background suppression, the signal-to-noise ratio improved a great deal, and I_{SFG} has a known dependence on N; it is precisely proportional to N^2.

Interpretation of SFG spectra of polyatomic molecules is a complicated matter, so for the purposes of understanding the SFG spectra of substituted benzene SAMs, we offer here a simple and useful approximate view useful for CH-stretching transitions. Let us use a local oscillator basis set and let the dipole moment lie along the bond direction. The polarizability has nonvanishing diagonal and off-diagonal elements[38] and is much more isotropic than the dipole moment, so for simplicity, we will consider only the dipole. In ordered upright monolayers of AT molecules, it is well-known that the SFG spectrum shows three methyl CH-stretching transitions.[37] The methylene (CH_2) transitions are weak. In our picture, this is easily understood: in an all-trans conformation, the dipoles of pairs of adjacent CH_2 groups exactly cancel. In BT, our picture suggests that in the SFG spectrum, the CH group at the 4-position will be dominant; the dipoles from CH groups at the 2,5- and 3,6-positions should cancel. In 4MBT, the CH-stretching transitions of the methyl group will be dominant since the four phenyl CH-stretch dipoles will again cancel. However, in asymmetric 2MBT or 3MBT, one would expect to see both methyl and phenyl CH-stretching transitions.

Experimental Procedures

The experimental method has been discussed previously in detail.[1,2,35] Here, we will give an outline plus a more detailed discussion of recently introduced improvements.

The samples, as before,[1,2,35] were fabricated on 50 mm × 50 mm × 1.6 mm glass substrates. Electron-beam evaporation was

used to deposit a 0.8 nm thick Cr adhesion layer and a 50 nm thick layer of Au. The coated substrates were soaked for several hours in an ethanol solution of the thiols, all of which were obtained from Aldrich Chemical. The samples were washed extensively in water and ethanol and mounted on a rotating sample holder.

The laser apparatus, based on a 3 mJ, 120 fs, kHz Ti:sapphire chirped-pulse amplifier, is diagrammed in Figure 1c. The NBVIS pulses were created by passing an 800 nm pulse of 120 fs duration through a Fabry−Perot étalon (TecOptics) with an air gap d of 11.1 μm, free-spectral range of 450 cm^{-1}, and finesse of 44 to produce a time asymmetric picosecond pulse with $\Delta\nu = 10.3$ cm^{-1}.[34] The NBVIS pulse energy was 15 μJ, focused with a 75 cm lens to a 300 μm beam diameter. The NBVIS pulses were incident on the sample at a 60° angle.

The BBIR pulses were 200 fs in duration and centered near 3.3 μm with an energy of 5−10 μJ. The spectral fwhm was ∼150 cm^{-1}. A 7.5 cm ZnSe lens was used to focus the beam to a ($1/e^2$) beam diameter of 200 μm.

The flash-heating pulses were created by picking off a portion of the Ti:sapphire laser amplified output prior to pulse compression. This stretched ∼100 ps pulse was directed through a second pulse compressor. By detuning this compressor, the flash-heating pulse duration could be varied from 100 fs to several ps. A longer duration minimizes nonlinear propagation effects through the glass substrates[45,46] but degrades the time resolution. A 300 fs duration was a good compromise. Astigmatism in the optical system produced a 2:1 elliptical beam profile that coincidently matched the elliptical footprint of the SFG beams at the sample. The flash-heating pulse was focused on a spot somewhat larger than the region probed by SFG, approximately 500 μm in length and 250 μm in height. The intensity of the flash-heating pulse was varied in the 100 μJ range to locate the threshold for melting Au, and then the pulse was attenuated by 20%.[1,2] Since the melting temperature (T_m) of Au was 1064 °C, this procedure resulted in flash-heating of the Au layer to ∼800 °C. Studies reported earlier[1,2] that measured thermally induced reflectance changes in the sample[47] indicated that there was a fast jump of the Au surface temperature to 80% of the final temperature within 1 ps, followed by a slower (1.5 ps time constant) rise to the final temperature. The slower part of the rise resulted mainly from heat flow from Cr into the Au layer.[1]

In the three-beam arrangement shown in Figure 1c, two SFG signals were generated. The first SFG resulted from the femtosecond BBIR and picosecond NBVIS pulses, and it produced the frequency-resolved adsorbate vibrational spectra. This signal was sent through the spectrograph onto the upper half of the CCD detector. The second SFG signal resulted from the femtosecond heating pulses and the femtosecond BBIR pulses interacting in the thin Au layer. This NR reference signal was sent through the spectrograph onto the lower half of the CCD. As the heating pulse was time-delayed, the reference accurately determined the laser apparatus time response and precisely located $t = 0$, which is defined as the instant that the peak of the flash-heating pulse arrived at the (very thin) Au layer.

This arrangement incorporated quite a few incremental improvements besides SFG background suppression, which have greatly improved our signal-to-noise ratio: (1) Since the SAM CH-stretching transitions are 10−15 cm^{-1} fwhm, we used an étalon with a 10 cm^{-1} transmission peak, rather than the 5 cm^{-1} peak used previously. This quadruples the NBVIS intensity since the transmitted pulse has twice the bandwidth, giving twice the energy and one-half the duration. (2) The dichroic beam combiner was eliminated by using separate focusing lenses for the NBVIS and BBIR beams. This allows us to use ZnSe for the IR lens, which produces a much better spot than CaF_2 used previously for the IR and visible beams. A significant problem with noncollinear beams has been that when the IR pulse frequency is tuned, phase matching caused the direction of the SFG signal to vary, which necessitated a realignment of the detection system. However, the spectrograph and CCD are insensitive to deflections along the vertical axis that runs parallel to the entrance slit. Our new setup takes advantage of this. The BBIR pulses were slightly offset in the vertical direction, slightly out of the horizontal plane of the incident and reflected NBVIS pulses, so that as the BBIR pulses were tuned, the SFG signal continued to fall onto the CCD detector. (3) The use of a second pulse compressor, as depicted in Figure 1c, allowed us more freedom in finding the best flash-heating pulse duration, it resulted in higher pulse energies, and by reducing the thermal load on the high-power compressor grating, the beam quality was improved. (4) The dual-beam arrangement with a signal and reference SFG signal improved our accuracy in determining $t = 0$ and measuring small propagation delays in heat arrival at different molecular locations.

Results

SFG Spectra. Figure 3a,b illustrates the effects of SFG background suppression, using a 16 carbon AT SAM as an example. The ordinary SFG spectrum shown in Figure 3a is well-known, consisting of a broad NR background having three sharper dips representing the three CH-stretching transitions of the terminal CH_3 groups, plus two quite weak methylene transitions.[3] With the time delay between BBIR and NBVIS pulses set at ∼600 fs, the NR-suppressed spectra in Figure 3b were obtained. The spectra with dashed lines in Figure 3a,b were obtained 20 ps after a temperature jump. The intensity changes due to flash-heating are easily seen.

Background-suppressed SFG spectra from benzenethiolate SAMs are shown in Figure 3c−e. Recall that methyl CH-stretching transitions are generally at 2900−2950 cm^{-1}, as compared to ∼3050 cm^{-1}, for phenyl CH-stretches. The BT spectrum[1,35] is dominated by a phenyl CH-stretching transition at 3050 cm^{-1}, which according to the previous discussion is attributed primarily to the 4-position CH-stretching oscillator. This cancellation is confirmed by the 4MBT spectrum in Figure 3d. The three methyl CH-stretching transitions of 4MBT are clearly evident, while no phenyl CH-stretching transitions are seen, even though there are still four remaining phenyl CH-stretching units. With the asymmetric 2MBT, both methyl and phenyl CH-stretching transitions can be seen in Figure 3e. We do not know why, but with 3MBT, the samples we made were oily and cloudy, and we did not obtain a good SFG spectrum.

Time Dependence: Vibrational Response Functions. To characterize the time-dependent response to flash-heating, the best signals were obtained from intensity changes in the most intense SFG transitions. To compare the response of different SAMs, we defined a normalized vibrational response function (VRF)[2,25,35]

$$\mathrm{VRF}(t) = [I(T_{\mathrm{cold}}) - I(t)]/[I(T_{\mathrm{cold}}) - I(T_{\mathrm{hot}})] \qquad (4)$$

where $I(T_{\mathrm{cold}})$ is the SFG intensity at ambient temperature, and $I(T_{\mathrm{hot}})$ is the intensity at 100 ps when Au and SAM have equilibrated. When a NR background is present, these intensities were the depth of the dips such as in Figure 3a; with NR suppression, these intensities are the peak heights.

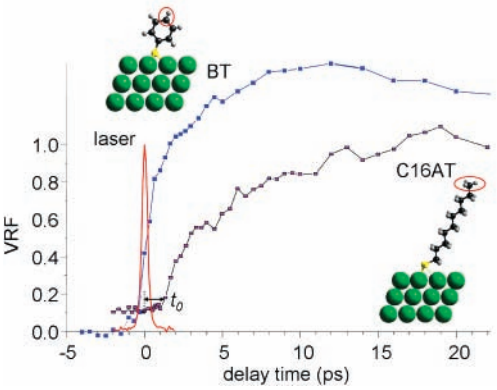

Figure 4. VRF for BT and 16-carbon AT SAMs resulting from flash-heating to ~800 °C. The data were normalized to a value of unity at long delay times (not shown), and the C16 data were offset by +0.1 for clarity. The curve denoted laser is the apparatus response measured as the cross-correlation between the femtosecond BBIR pulses and the femtosecond flash-heating pulses. The VRF of the AT SAM evidences a delay time t_0 resulting from the time needed for the heat burst to propagate along the alkane chain.

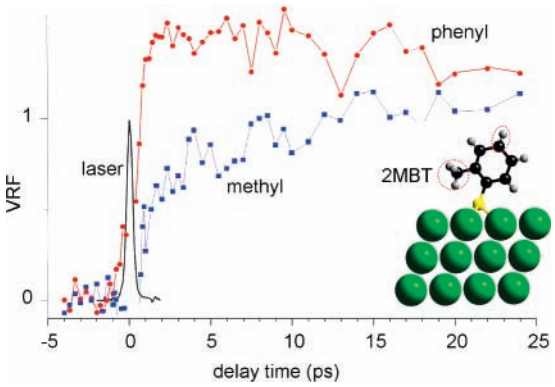

Figure 5. VRF for 2MBT in the phenyl CH-stretching and methyl CH-stretching regions. The data were normalized to a value of unity at long delay times (not shown). The short-time transients show that the phenyl signal rise is approximately a step function. The methyl signal rise is about equal parts step function and a slower component.

To better characterize the improved flash-heating apparatus, we remeasured the AT and BT SAMs. The results are shown in Figure 4. With BT, where SFG probes the CH unit at the 4-position, the rise of the VRF is very fast. In fact, the short-time VRF quite closely mirrors what was measured by time-resolved reflectivity methods for the surface temperature jump,[1] namely, an ~1 ps jump to ~80% of the final temperature followed by an exponential rise to the final temperature with a 1.5 ps time constant. The long-time part of the BT VRF has an unusual behavior.[1] It overshoots the long-time limiting value of unity, rising above unity in the 5−40 ps time range. This overshoot means that when the flash-heating pulse arrives, the SFG intensity drops dramatically, and then it partially recovers before settling into equilibrium at the higher temperature. This behavior was discussed in another publication,[1] where we explained that it seemed impossible to attribute the overshoot behavior to heat flow alone since the metal surface is at a high temperature that remains constant during the time of observation. Instead, we believe that this overshoot results from a thermally induced structural relaxation process. The low-temperature structure has, according to the simulations of Jung et al.,[48] a great deal of built-in strain due to a lack of conformational freedom of the Au−S−phenyl bond. This prevents the phenyl groups from forming the sandwich configuration or the even better T-shaped configuration. At higher temperatures, we speculated that the phenyl groups can adopt more favorable orientations. But here, we primarily were concerned with the short-time transient response, and this transient response is very fast indeed.

The results obtained with the 16 carbon AT, where SFG selectively probed the terminal methyl group, agree well with what was reported previously.[2] The build-up of the VRF with a 5 ps time constant is indicative of the interface conductance limited time for the chains to come into equilibrium with the hot Au surface. A remarkable short-time transient effect is also seen. This is a delay of $t_0 = 1.2$ ps before the molecular response begins to turn on. This delay time was interpreted as the time for the leading edge of the heat burst to move from the Au surface to the base of the alkane chains (the base is a region of four to five carbon atoms ~0.8 nm in length) and then to propagate along the 2.4 nm long C16 chains to the terminal methyl groups.[2]

2MBT. For 2MBT, we measured VRFs for both phenyl and methyl CH-stretching transitions, as shown in Figure 5. The phenyl signal is similar to what was observed for BT, except the rise is even a bit steeper. In fact, the short-time part of the phenyl VRF is practically a step function. The methyl VRF has a two-part rise, with each part accounting for about one-half of the total rise. The faster part is quite similar to the rise of the phenyl signal. The remaining part of the methyl VRF is clearly slower than what is seen when the phenyl groups are probed. In other words, VRFs that observe different parts of the 2MBT molecule reveal clearly different dynamics.

Discussion

Origin of VRF. The loss of SFG intensity represented by the VRF can result from two possible causes.[1] The first is a single-molecule property. As molecules heat up, the thermally averaged SFG cross-section will change, and generally, this change would be in the direction of a lower cross-section. The second is an ensemble property. SFG is a coherent process that depends on the ensemble average of $\mu(0)\alpha(t)$, so thermally induced disorder will decrease both the ensemble-averaged dipole moment and the polarizability.

The time dependence of SFG intensity loss similarly can result from two possible sources, the rate of heat flow into the molecules or the rate at which the molecules respond to heating.[1] When the metal surface is heated, vibrational energy flows from the metal substrate into the lower energy molecular vibrations. A change in the SFG intensity from the higher frequency CH-stretching vibrations will occur as a result of intramolecular anharmonic coupling. These lower energy vibrational excitations also may cause structural relaxation in the form of thermally induced disordering. Our viewpoint, expressed previously,[1] is that both the anharmonic interactions and the structural disordering are faster than the heat flow, so that the time dependence of the VRF should be interpreted as resulting from heat flow into the SAM molecules. This view was put forth in our study of AT chains[1] on the basis of nonequilibrium MD simulations. We showed that with instantaneous heating, molecular disordering occurred within about 1 ps, so a VRF evidencing time constants slower than 1 ps should be interpreted as denoting heat flow into the SAM molecules.

Energy Flow in 2MBT. The data in Figure 5 from 2MBT show a two-part VRF for the methyl groups with one part noticeably slower than what is seen for the phenyl groups. Interpreting the VRF as resulting from heat flow-induced

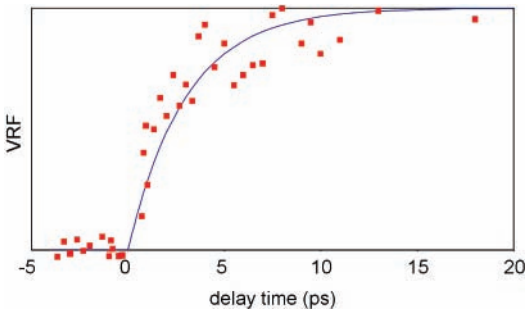

Figure 6. Slower component of the VRF for 2MBT derived from the data in Figure 5 by determining that 1 − [phenyl(t) − methyl(t)] is a good fit to an exponential rise with a time constant $\tau/2$ of 4 ps. Heat flow from the thiolate linkage, through the phenyl group to the methyl group, takes 8 ps.

thermal disordering leads to the following picture. The fast initial rush of heat into the phenyl groups, via the thiolate linkages, causes an increase in the thermal amplitude of phenyl group motions. Since the phenyl moiety is basically rigid, the relevant motions might be torsions of the Au−S and S−C bonds. Ultrafast heating creates an orientationally disordered benzene monolayer. Notice that to create disorder, there need not be any heat flow into the phenyl groups themselves, just into the thiolate linkage, which accounts for the fast rise time for the phenyl VRF. As the cold phenyl rings undergo orientational disorder, the methyl substituents also become disordered, as they are passengers on the phenyl rings. But, there is also a slower part of the methyl VRF that we attribute to additional methyl disorder created by heat flow into the methyl groups. Since the SAM is a densely packed 2-D layer, the potential landscapes for the methyl groups undoubtedly have multiple minima. When heat flows into the methyl groups, there will be enhanced motions involving C−C bending and rotation around the C−C bond, which would allow the methyl groups to sample additional configurations.

To assign a time constant to the process of rate of heat flow into the thiolate linkage, through the phenyl ring into the methyl, which is responsible for the slower component of methyl disordering, we made the plot shown in Figure 6, which has the form $f(t) = 1 - [\text{phenyl}(t) - \text{methyl}(t)]$. Since the phenyl VRF is noisy but almost a step function, we actually approximated the phenyl VRF as a step function. As shown in Figure 6, the result is a good fit to an exponential build-up function $f(t) = 1 - \exp(-2t/\tau)$, where the factor 2 arises due to the N^2 dependence of the VRF with background suppression. The time constant τ is 8 (±2) ps, where the error bound is based on goodness-of-fit.

Conclusion

For the first time, we observed heat flow through a layer of molecules where the heat is the input from one location, and its effects were probed in real time at two different locations. As heat flows from the hot metal surface into the 2MBT SAM layer, phenyl disordering occurs promptly, as a result of thermal excitation of the thiolate linkage. Subsequently, heat flow into the phenyl groups and to the 2-methyl substituent causes methyl disordering. Thus, the methyl VRF has two parts: a faster part representing the creation of disorder due to phenyl motions and a slower 8 ps part representing the creation of disorder due to thermal excitation of the methyl groups. Since methyl torsions and librations are much faster than 8 ps, 8 ps is interpreted as the time for heat to flow from the thiolate linkage, through the phenyl groups, and into the methyl substituents.

Acknowledgment. This material is based upon work supported by the National Science Foundation under Award DMR 0504038, the Air Force Office of Scientific Research under Award FA9550-06-1-0235, and the Army Research Office under Awards W911NF-05-1-0345 and W911NF-04-1-0178.

References and Notes

(1) Wang, Z.; Cahill, D. G.; Carter, J. A.; Koh, Y. K.; Lagutchev, A.; Seong, N.-H.; Dlott, D. D. *Chem. Phys.* **2008**, doi: 10.1016/j.chemphys.2007.12.017.
(2) Wang, Z.; Carter, J. A.; Lagutchev, A.; Koh, Y. K.; Seong, N.-H.; Cahill, D. G.; Dlott, D. D. *Science (Washington, DC, U.S.)* **2007**, *317*, 787.
(3) Richter, L. J.; Petralli-Mallow, T. P.; Stephenson, J. C. *Opt. Lett.* **1998**, *23*, 1594.
(4) Schwarzer, D.; Hanisch, C.; Kutne, P.; Troe, J. *J. Phys. Chem. A* **2002**, *106*, 8019.
(5) Schwarzer, D.; Kutne, P.; Schröder, C.; Troe, J. *J. Chem. Phys.* **2004**, *121*, 1754.
(6) Chen, S.; Seidel, M. T.; Zewail, A. H. *Angew. Chem., Int. Ed.* **2006**, *45*, 5154.
(7) Seidel, M. T.; Chen, S.; Zewail, A. H. *J. Phys. Chem. C* **2007**, *111*, 4920.
(8) Yang, D.-S.; Gedik, N.; Zewail, A. H. *J. Phys. Chem. C* **2007**, *111*, 4889.
(9) Smits, M.; Ghosh, A.; Bredenbeck, J.; Yamamoto, S.; Müller, M.; Bonn, M. *New J. Phys.* **2007**, *9*, 390.
(10) Segal, D.; Nitzan, A. *J. Chem. Phys.* **2002**, *117*, 3915.
(11) Segal, D.; Nitzan, A.; Hänggi, P. *J. Chem. Phys.* **2003**, *119*, 6840.
(12) Smalley, J. F.; Finklea, H. O.; Chidsey, C. E. D.; Linford, M. R.; Creager, S. E.; Ferraris, J. P.; Chalfant, K.; Zawodzinsk, T.; Feldberg, S. W.; Newton, M. D. *J. Am. Chem. Soc.* **2003**, *125*, 2004.
(13) Segal, D.; Nitzan, A. *J. Chem. Phys.* **2005**, *122*, 104704.
(14) Segal, D.; Nitzan, A. *Phys. Rev. E: Stat., Nonlinear, Soft Matter Phys.* **2006**, *73*, 26109.
(15) Galperin, M.; Ratner, M. A.; Nitzan, A. *J. Phys.: Condens. Matter* **2007**, *19*, 103201.
(16) Kabadi, V. N.; Rice, B. M. *J. Phys. Chem. A* **2004**, *108*, 532.
(17) Kim, H.; Dlott, D. D. *J. Chem. Phys.* **1991**, *94*, 8203.
(18) Nguyen, P. H.; Stock, G. *J. Chem. Phys.* **2003**, *119*, 11350.
(19) Hopkins, J. B.; Powers, D. E.; Mukamel, S.; Smalley, R. E. *J. Chem. Phys.* **1980**, *72*, 5049.
(20) Reddy, K. V.; Heller, D. F.; Berry, M. J. *J. Chem. Phys.* **1982**, *76*, 2814.
(21) Heilweil, E. J.; Casassa, M. P.; Cavanagh, R. R.; Stephenson, J. C. *Annu. Rev. Phys. Chem.* **1989**, *40*, 143.
(22) Pang, Y.; Deàk, J. C.; Huang, W.; Lagutchev, A.; Pakoulev, A.; Patterson, J. E.; Sechler, T. D.; Wang, Z.; Dlott, D. D. *Int. Rev. Phys. Chem.* **2007**, *26*, 223.
(23) Wang, Z.; Pakoulev, A.; Dlott, D. D. *Science (Washington, DC, U.S.)* **2002**, *296*, 2201.
(24) Patterson, J. E.; Lagutchev, A. S.; Hambir, S. A.; Huang, W.; Yu, H.; Dlott, D. D. *Shock Waves* **2005**, *14*, 391.
(25) Patterson, J. E.; Lagutchev, A. S.; Huang, W.; Dlott, D. D. *Phys. Rev. Lett.* **2005**, *94*, 15501.
(26) Nuzzo, R. G.; Zegarski, B. R.; Dubois, L. H. *J. Am. Chem. Soc.* **1987**, *109*, 733.
(27) Alara, D. L.; Nuzzo, R. G. *Langmuir* **1985**, *1*, 52.
(28) Ge, Z. B.; Cahill, D. G.; Braun, P. V. *Phys. Rev. Lett.* **2006**, *96*, 186101.
(29) Putnam, S. A.; Cahill, D. G.; Braun, P. V. *J. Appl. Phys.* **2006**, *99*, 84308.
(30) Wang, R. Y.; Segalman, R. A.; Majumdar, A. *Appl. Phys. Lett.* **2006**, *89*, 173113.
(31) Cahill, D. G.; Ford, W. K.; Goodson, K. E.; Mahan, G. D.; Majumdar, A.; Maris, H. J.; Merlin, R.; Phillpot, S. R. *J. Appl. Phys.* **2003**, *93*, 793.
(32) Bain, C. D.; Troughton, E. B.; Tao, Y.-T.; Evall, J.; Whitesides, G. M.; Nuzzo, R. G. *J. Am. Chem. Soc.* **1989**, *111*, 321.
(33) Ge, Z.; Cahill, D. G.; Braun, P. V. *J. Phys. Chem. B* **2004**, *108*, 18870.
(34) Lagutchev, A.; Hambir, S. A.; Dlott, D. D. *J. Phys. Chem. C* **2007**, *111*, 13645.
(35) Lagutchev, A. S.; Patterson, J. E.; Huang, W.; Dlott, D. D. *J. Phys. Chem. B* **2005**, *109*, 5033.
(36) Patterson, J. E.; Dlott, D. D. *J. Phys. Chem. B* **2005**, *109*, 5045.
(37) Harris, A. L.; Chidsey, C. E. D.; Levinos, N. J.; Loiacono, D. N. *Chem. Phys. Lett.* **1987**, *141*, 350.
(38) Shen, Y. R. *The Principles of Nonlinear Optics*; Wiley: New York, 1984.

(39) Shen, Y. R. *Nature (London, U.K.)* **1989**, *337*, 519.
(40) Shen, Y. R. *Surf. Sci.* **1994**, *299*−*300*, 551.
(41) Perry, A.; Niepert, C.; Space, B.; Moore, P. B. *Chem. Rev.* **2006**, *106*, 1234.
(42) Eisenthal, K. B. *Annu. Rev. Phys. Chem.* **1992**, *43*, 627.
(43) Eisenthal, K. B. *Chem. Rev.* **1996**, 1343.
(44) Lu, G. Q.; Lagutchev, A.; Dlott, D. D.; Wieckowski, A. *Surf. Sci.* **2005**, *585*, 3.
(45) Huang, W.; Patterson, J. E.; Lagutchev, A.; Dlott, D. D. *AIP Conf. Proc.* **2006**, *845*, 1265.
(46) Moore, D. S.; Gahagan, K. T.; Reho, J. H.; Funk, D. J.; Buelow, S. J.; Rabie, R. L.; Lippert, T. *Appl. Phys. Lett.* **2000**, *78*, 40.
(47) Cahill, D. G. *Rev. Sci. Instrum.* **2004**, *75*, 5119.
(48) Jung, H. H.; Won, Y. D.; Shin, S.; Kim, K. *Langmuir* **1999**, *15*, 1147.